Abstract A formulation of the perturbed two-body problem that relies on a new set of orbital elements is presented. The proposed method represents a generalization of the special perturbation method published by Peláez et al. (Celest Mech Dyn Astron 97(2):131–150, 2007) for the case of a perturbing force that is partially or totally derivable from a potential. We accomplish this result by employing a generalized Sundman time transformation in the framework of the projective decomposition, which is a known approach for transforming the two-body problem into a set of linear and regular differential equations of motion. Numerical tests, carried out with examples extensively used in the literature, show the remarkable improvement of the performance of the new method for different kinds of perturbations and eccentricities. In particular, one notable result is that the quadratic dependence of the position error on the time-like argument exhibited by Peláez's method for near-circular motion under the J_2 perturbation is transformed into linear. Moreover, the method reveals to be competitive with two very popular element methods derived from the Kustaanheimo-Stiefel and Sperling-Burdet regularizations.

Keywords Perturbed two-body problem · Regularization · Generalized orbital elements · Orbit propagation · Linearization

1 Introduction

The most straightforward method for finding the solution of the perturbed two-body problem is known in Celestial Mechanics as Cowell's method (Battin 1999, p. 447), which consists

G. Baù (✉)
CISAS "G. Colombo", University of Padova, Via Venezia 15, 35131 Padova, Italy
e-mail: bagiugio@gmail.com

C. Bombardelli · J. Peláez
Space Dynamics Group, School of Aeronautics, Technical University of Madrid,
Plaza Cardenal Cisneros 3, 28040 Madrid, Spain

of a direct integration of the Newtonian equations of motion in rectangular coordinates. Unfortunately, these differential equations become singular when the distance between the two bodies, regarded as point masses, becomes zero. Even if such a condition is unrealistic because bodies have a finite size, the numerical method suffers from loss of accuracy in situations approaching the singular case.

The elimination of singularities occurring in the equations of motion by properly selected variables is called *regularization* and leads to a set of regular differential equations (Szebehely 1975). The first fundamental lines of research in this field were pursued by Levi-Civita (1924) and Sundman (1907, 1912) on the regularization of the three-body problem.

A very desirable property that often accompanies regularization is *linearization* (Deprit et al. 1994). When linearization is obtained the transformed equations of motion of the perturbed two-body problem take the form of perturbed harmonic oscillators with improved stability properties, and, as a result, improved numerical propagation performance not only for the case of near-collision orbits (like for instance highly eccentric ellipses), but in general of any kind of motion (Arakida and Fukushima 2000). On the contrary, Cowell's equations for the two-body problem are nonlinear and the solution is Lyapunov-unstable (Stiefel and Scheifele 1971, Section 16; Bond 1982).

The natural way of obtaining regularization is to transform the independent and/or dependent variables and to introduce integrals into the equations of motion (Bond and Allman 1996, Chap. 9). The three most popular regularization schemes developed for the three-dimensional perturbed two-body problem are known as the Kustaanheimo-Stiefel (K-S) (Kustaanheimo and Stiefel 1965), the Sperling-Burdet (S-B) (Sperling 1961; Burdet 1967), and the Burdet-Ferrándiz (B-F) (Burdet 1969; Ferrándiz 1987/88) regularization.

As a first step towards regularization the above methods perform a change in the independent variable from physical time to a different independent variable sometimes referred to as *fictitious time*. For the K-S and S-B methods the independent variable has the dimension of an inverse velocity by virtue of a Sundman's time transformation, while the B-F method uses an angular variable that coincides with the true anomaly in the unperturbed motion. Following this change of variable, each of the schemes adopts its own approach towards full regularization. The K-S regularization extends in a four-dimensional parametric space the planar transformation of Levi-Civita (Stiefel and Scheifele 1971, Chap. 2). The S-B regularization is achieved by embedding the Laplace vector and the Keplerian energy into the equations of motion written with respect to the new independent variable (Bond and Allman 1996, Section 9.3). The B-F regularization exploits a *projective decomposition* of the equations of motion in which the dynamics of the orbital radius and the radial direction are considered separately (Fukushima 2007a), an idea already known since the eighteenth century and codified by Laplace (Deprit et al. 1994).

A new two-body regularization has been recently proposed by Fukushima (2007a) employing only eight dependent variables. The Sundman's and Levi-Civita's time and space transformations respectively are combined to achieve regularization with respect to a coordinate triad representing the orbital plane. The orientation of this plane is given by integrals of the unperturbed motion, namely the components of the angular momentum vector in a fixed reference frame.

Following any of the the three regularization schemes described above a system of linear and regular second order differential equations is obtained (Fukushima 2007a). However, it is worth noting that only the B-F regularization relies on perturbed harmonic oscillators for any admissible value of the total energy (Chelnokov 1993) with the K-S and S-B regularizations exhibiting oscillator properties only in the case of total energy strictly smaller than zero.

A further improvement in numerical propagation performance can be obtained by applying the method of *variation of parameters* (VOP) (Vallado 2001, Section 9.3) whereby the dependent variables are transformed into orbital elements, which are held constant in the case of pure Keplerian motion. Because no discretization error affects the elements propagation in the unperturbed motion, methods that employ elements are especially suited to the propagation of celestial bodies as well as artificial satellites subject to relatively weak perturbations. VOP formulations have been developed for the K-S, S-B and B-F regularizations. In the framework of the K-S regularization, the first set of elements was derived for perturbed elliptic motion by Stiefel in 1967 (Stiefel et al. 1967; Arakida and Fukushima 2001) and subsequently modified by Stiefel and Scheifele (1971, Section 19), who also presented (Stiefel and Scheifele 1971, Section 40) K-S elements valid in any kind of orbit but only when the perturbing force arises from a potential. This limitation motivated Bond (1974) to find the solution of the K-S transformed perturbed two-body problem in terms of a uniform set of elements working for perturbations both derivable and not derivable from a potential. Arakida and Fukushima (2001) have shown that the use of elements under the K-S regularization significantly reduces the error propagation in the numerical integration of the differential equations of motion. In the S-B scheme, Burdet (1967, 1968) applied the VOP technique to Sperling's regularization to obtain the differential equations of the elements which appeared in Sperling's solution. Burdet's approach was then modified by Bond and Fraietta who introduced spatial and temporal elements (Bond and Allman 1996, Chap. 9).

As regards the B-F regularization, a VOP method has been recently developed by (Peláez et al. 2007). The method, which was presented for the first time in 2005 (Peláez et al. 2005), is often referred to as *Dromo* [1] and is characterized by eight dependent variables: the physical time, the inverse of the angular momentum, two elements related to the dynamics along the radial direction and the four components of a unit quaternion describing the attitude of a slowly moving frame. Such a frame is known after Hansen (1857) as an *ideal* frame, and it was also exploited by Deprit (1975) for determining a set of ideal elements which show a strong analogy with Peláez's elements. When compared to other propagation schemes Dromo has been shown to offer a number of important advantages: non-degenerate quaternion differential equations, compact form of the equations of motion with perturbing accelerations appearing directly in a local-vertical local-horizontal orbiting frame, a reduced number of equations to be integrated (a total of eight variables is employed, two less than the K-S formulation), a unique formulation for the three types of perturbed conics with no need for embedding Stumpff functions. Furthermore, the method has been used to derive the first complete asymptotic solution (i.e. including secular and periodic terms) of the two-body problem perturbed by constant tangential thrust (Bombardelli et al. 2011).

Although the Dromo formulation has been shown to offer an excellent numerical propagation performance, its computational speed and/or propagation accuracy can still be improved. In its current formulation, for instance, the method cannot benefit from the performance increase that is normally achievable when the perturbing force is partially or fully derivable from a potential. In fact, both the K-S and S-B formulations take advantage of this situation by introducing the total energy (Stiefel and Scheifele 1971, p. 30; Bond and Hanssen 1973) or the Jacobi integral (Bond and Gottlieb 1989) instead of the Keplerian energy as dependent variable. In such case, conservative potentials rather than their corresponding perturbing forces should be inserted in the equations of motion whenever possible (Stiefel and Scheifele 1971, p. 117).

[1] The word *dromo* is derived from the old Greek word δρόμος (dròmos) that means *running*.

The aim of this paper is to generalize the Dromo propagation method to account for disturbing potentials. This is done by adopting the *generalized Sundman time transformation* as it was presented by Sharaf et al. (1992) for the particular case of order two, where the angular momentum is replaced by what we call a "pseudo angular momentum". The new set of generalized orbital elements proposed here inherits all the benefits of Dromo elements, in particular they are nonsingular for all eccentricities and inclinations and provide a uniform solution of the perturbed two-body problem, in the sense that the same solution is valid for all values of the energy. In addition, and this is the main contribution of this work, they show a much better numerical behavior when conservative potentials are considered.

In Sect. 2 we derive the linear differential equations of the perturbed two-body problem. In Sect. 3 we apply the VOP technique to such equations in order to derive the new set of elements and their differential equations. In Sect. 4 we provide a physical interpretation of the new elements by establishing relations with the classical orbital elements as well as with the Cartesian components of the position and velocity vectors. Finally, we exploit some extensively used examples in the literature to compare the performance of our method with respect to the classical version of Dromo and two well known VOP methods belonging to the K-S and S-B regularization schemes.

2 Linearized equations of motion

Let us consider a particle of mass m orbiting around a primary of mass M at initial radial position R_0 measured from the center of the primary and angular position ν_0 measured from the initial eccentricity vector (and hence corresponding to the initial true anomaly). Let us employ, from now on, m as the unit of mass, R_0 as the unit of distance and $1/n_0$ as the unit of time where n_0 is the angular rate of a *circular* orbit with radius equal to the initial radius R_0:

$$n_0 = \sqrt{\frac{G\,(M+m)}{R_0^3}},$$

with G denoting the gravitational constant. In the following we will always refer to non-dimensional quantities, unless otherwise stated.

The evolution of the particle m obeys the perturbed two-body problem equation written here in the non-dimensional form:

$$\frac{\mathrm{d}^2\mathbf{r}}{\mathrm{d}t^2} = -\frac{1}{r^3}\mathbf{r} + \mathbf{f}, \tag{1}$$

where $\mathbf{r}$ is the position of the particle with respect to the primary and $\mathbf{f}$ is the perturbing force applied to the particle. The latter can be written as the sum of two contributions:

$$\mathbf{f} = \mathbf{P} - \frac{\partial \mathcal{U}\,(t,\ \mathbf{r},\ \mathbf{v})}{\partial \mathbf{r}},$$

with $\mathcal{U}$ denoting the perturbing potential energy, which, in general, is a scalar function depending on time t, $\mathbf{r}$ and the velocity $\mathbf{v}$ of the particle, and $\mathbf{P}$ indicating the perturbing force that is not derived by a perturbing potential energy. Once Eq. (1) has been double-integrated with the initial conditions $\mathbf{r}\,(0)$ and $\mathbf{v}\,(0)$ the position $\mathbf{r}\,(t)$ is known at a generic time t.

In this paper the motion is obtained by considering separately the dynamics of the inverse of the orbital distance $1/r$ and the radial direction $\mathbf{r}/r$. Such a coordinate transformation is applied together with a transformation of the independent variable from the physical time t to a fictitious time ϕ, which is shown in Subsect. 2.1. In the new space and time variables

Eq. (1) can be substituted by a set of linear (at least when the motion is unperturbed) differential equations, as it is described in Subsect. 2.2.

2.1 Generalized Sundman time transformation

A Sundman time transformation, coinciding with the angular momentum variation equation, is employed by the Dromo method (Peláez et al. 2007) to relate the physical time t with a new independent variable σ:

$$\frac{\mathrm{d}t}{\mathrm{d}\sigma} = \frac{r^2}{h}, \tag{2}$$

where r and h are the orbital radius and angular momentum of osculating Keplerian motion, respectively. The latter quantity can always be written as:

$$h = r\sqrt{v^2 - \left(\frac{\mathrm{d}r}{\mathrm{d}t}\right)^2} = r\sqrt{2\left(\varepsilon_K + \frac{1}{r}\right) - \left(\frac{\mathrm{d}r}{\mathrm{d}t}\right)^2}, \tag{3}$$

where:

$$\varepsilon_K = \frac{v^2}{2} - \frac{1}{r}$$

is the Keplerian energy, with v denoting the velocity magnitude.

Let us now introduce the *pseudo angular momentum*:

$$\tilde{h} = r\sqrt{2\left(\varepsilon + \frac{1}{r}\right) - \left(\frac{\mathrm{d}r}{\mathrm{d}t}\right)^2}, \tag{4}$$

where we formally added to the Keplerian energy the disturbing potential energy $\mathcal{U}$ to obtain the total energy:

$$\varepsilon = \varepsilon_K + \mathcal{U}.$$

By replacing h with $\tilde{h}$ in Eq. (2) we obtain the generalized Sundman transformation of order two as defined by Sharaf et al. (1992):

$$\frac{\mathrm{d}t}{\mathrm{d}\phi} = \frac{r^2}{\tilde{h}}. \tag{5}$$

By comparing Eqs. (3) and (4) we infer that:

$$\tilde{h} = \sqrt{h^2 + 2r^2\mathcal{U}}. \tag{6}$$

Unlike Eq. (2) which is just the expression of the orbital angular momentum, Eq. (5) does not have a straightforward physical meaning. On the other hand, it is instructive to relate the independent variable ϕ to well known astrodynamical quantities such as the classical orbital elements. To this end, let us write the variation of the independent variable ϕ with respect to the initial value ϕ_0 as the sum:

$$\Delta\phi = \Delta\nu + \gamma, \tag{7}$$

where $\Delta\nu = \nu - \nu_0$, being ν the true anomaly. The latter quantity takes the expression (as shown in Appendix II which is published as Electronic Supplementary Material):

$$\gamma = \Delta\omega + \int_{\Omega_0}^{\Omega} \cos i \, \mathrm{d}\Omega + 2 \int_0^t \frac{\mathcal{U}}{\tilde{h} + h} \, \mathrm{d}t,$$

where $\Delta\omega$, Ω and i are, respectively, the argument of periapsis variation with respect to the initial orbit, the longitude of the ascending node and the orbital inclination. Equation (7) underlines that the variation $\Delta\phi$ of the independent variable differs, in general, from the variation $\Delta\nu$ of the osculating true anomaly by an *angular drift* γ due to the action of orbital perturbations. Therefore, ϕ can be referred to as *pseudo true anomaly* of the perturbed orbital motion.

In the particular case in which the orbital plane is invariant ($\Omega = \Omega_0$) and $\mathcal{U} = 0$, γ coincides with the angle between the eccentricity vector of the initial and of the osculating orbit, and ϕ, after setting $\phi_0 = \nu_0$, becomes the longitude of the particle measured from the eccentricity vector of the initial orbit. The initial value of the independent variable is arbitrary. In our implementation of the method the value of the initial true anomaly ν_0 was assigned to ϕ_0, so that $\phi_0 = \nu_0$.

2.2 Projective decomposition

Let us express the position $\mathbf{r}$ as the product of its magnitude r and its direction $\mathbf{i}$, in order to decompose the motion of the particle into a displacement of magnitude r along the radial direction $\mathbf{i}$ and a rotation of $\mathbf{i}$. This procedure is known as *projective decomposition* (Ferrándiz 1987/88; Deprit et al. 1994).

We introduce a rotating frame $\mathcal{R} = \langle x, y, z \rangle$ with one axis oriented along the radial direction $\mathbf{i}$. Let the axes of $\mathcal{R}$ be defined as follows:

1. the x-axis is oriented along $\mathbf{i}$;
2. the y-axis is oriented along the unit vector $\mathbf{j}$ which lies on the osculating orbital plane, is perpendicular to $\mathbf{i}$ and satisfies the condition $\mathbf{j} \cdot \mathbf{v} \geq 0$, being $\mathbf{v}$ the velocity vector;
3. the z-axis is oriented along the direction $\mathbf{k}$ of the orbital angular momentum vector $\mathbf{h} = \mathbf{r} \times \mathbf{v}$.

According to the previous definitions, the orthonormal basis $\{\mathbf{i}, \mathbf{j}, \mathbf{k}\}$ is defined by the relations:

$$\mathbf{i} = \frac{\mathbf{r}}{r}, \qquad \mathbf{j} = \mathbf{k} \times \mathbf{i}, \qquad \mathbf{k} = \frac{\mathbf{h}}{h}. \tag{8}$$

Following the idea of the projective decomposition the particle's dynamics is described by the four projective coordinates $(r, \mathbf{i})$ and their time derivatives $(\mathrm{d}r/\mathrm{d}t, \mathrm{d}\mathbf{i}/\mathrm{d}t)$. Next, we will derive a set of *linear* equations of motions corresponding to the inverse of the orbital radius r, and the orbital radius direction expressed in quaternion form.

2.2.1 Orbital radius dynamics

The radial component of Eq. (1) can be written as:

$$\frac{\mathrm{d}^2 r}{\mathrm{d}t^2} - \frac{h^2}{r^3} + \frac{1}{r^2} = f_x, \tag{9}$$

where $f_x = \mathbf{f} \cdot \mathbf{i}$.

As shown by Szebehely and Bond (1983) Eq. (9) can be linearized (at least for the unperturbed case) by employing the following transformation of the orbital radius:

$$r = \rho^{-1}, \tag{10}$$

together with a suitable change in the independent variable. To this end we substitute Eqs. (10) and (5) into Eq. (9) to obtain, as detailed in Appendix II (published as Electronic Supplementary Material):

$$\frac{\mathrm{d}^2\rho}{\mathrm{d}\phi^2} + \rho - \frac{1}{\tilde{h}^2} = -\frac{1}{\tilde{h}}\frac{\mathrm{d}\rho}{\mathrm{d}\phi}\frac{\mathrm{d}\tilde{h}}{\mathrm{d}\phi} - \frac{1}{\rho\tilde{h}^2}\left(\frac{f_x}{\rho} - 2\mathcal{U}\right), \tag{11}$$

where the term $\mathrm{d}\tilde{h}/\mathrm{d}\phi$ takes the form:

$$\frac{\mathrm{d}\tilde{h}}{\mathrm{d}\phi} = \frac{1}{\rho^3\tilde{h}}\left[\frac{\mathrm{d}\rho}{\mathrm{d}\phi}\left(\rho\frac{\partial\mathcal{U}}{\partial\rho} - 2\mathcal{U}\right) + \frac{1}{\rho\tilde{h}}\left(P_y\sqrt{\rho^2\tilde{h}^2 - 2\mathcal{U}} + \frac{\partial\mathcal{U}}{\partial t}\right)\right], \tag{12}$$

being $P_y = \mathbf{P}\cdot\mathbf{j}$, which is derived in Appendix II (published as Electronic Supplementary Material). Note that when $f_x = P_y = \mathcal{U} = 0$ Eq. (11) represents a harmonic oscillator perturbed by the constant positive term h^{-2}.

2.2.2 Radial direction dynamics

The time variation of the radial unit vector $\mathbf{i}$ obeys in general:

$$\frac{\mathrm{d}\mathbf{i}}{\mathrm{d}t} = \frac{h}{r^2}\mathbf{j}.$$

From the above expression and taking into account Eqs. (5) and (6) one readily obtains:

$$\frac{\mathrm{d}\mathbf{i}}{\mathrm{d}\phi} = \sqrt{1 - \frac{2r^2\mathcal{U}}{\tilde{h}^2}}\,\mathbf{j}. \tag{13}$$

If both sides of this equation are differentiated with respect to ϕ it results a second order differential equation in ϕ which for vanishing $\mathcal{U}$ and f_z represents a harmonic oscillator in the state variable $\mathbf{i}$.

We propose instead to exploit Eq. (13) to replace $\mathrm{d}\mathbf{i}/\mathrm{d}\phi$ with $\mathbf{j}$ in the state vector. This implies that we have to consider also the pseudo angular momentum $\tilde{h}$ as a state variable.

Note that the two unit vectors $\mathbf{i}$ and $\mathbf{j}$ provide the evolution of the rotating frame $\mathcal{R}$ which was defined in Eq. (8). According to Euler's rotation theorem, the attitude of $\mathcal{R}$ with respect to a reference frame $\mathcal{I}$ with fixed orientation in space is obtained by a rotation of an angle φ around a unit vector $\mathbf{u}$. Following quaternion algebra, let us introduce the unit quaternion $\hat{q}$ associated to such rotation:

$$\hat{q} = (q_4,\ \mathbf{q}), \tag{14}$$

where the scalar part q_4 and the vectorial part $\mathbf{q}$ are functions of φ and $\mathbf{u}$ as follows:

$$q_4 = \cos\frac{\varphi}{2}, \qquad \mathbf{q} = \mathbf{u}\sin\frac{\varphi}{2}. \tag{15}$$

By projecting $\mathbf{q}$ onto the rotating frame $\mathcal{R}$ as:

$$\mathbf{q} = q_1\mathbf{i} + q_2\mathbf{j} + q_3\mathbf{k},$$

the time derivative of $\hat{q}$ appears in the form:

$$\frac{\mathrm{d}\hat{q}}{\mathrm{d}t} = \frac{1}{2}\hat{q}\,\hat{w},$$

where $\hat{q}\,\hat{w}$ represents the *quaternion product* of $\hat{q}$ by the quaternion $\hat{w} = (0,\ \mathbf{w})$ being $\mathbf{w}$ the angular velocity of the frame $\mathcal{R}$ which is represented in $\mathcal{R}$ by:

$$\mathbf{w} = \frac{rf_z}{h}\mathbf{i} + \frac{h}{r^2}\mathbf{k}.$$

After applying the quaternion product rule and switching from t to ϕ we have:

$$\frac{\mathrm{d}\hat{q}}{\mathrm{d}\phi} = \frac{r^2}{2\tilde{h}}\left(-\mathbf{q}\cdot\mathbf{w},\ q_4\mathbf{w} + \mathbf{q}\times\mathbf{w}\right),$$

which yields the four differential equations:

$$\frac{\mathrm{d}q_1}{\mathrm{d}\phi} = \frac{1}{2\rho\tilde{h}\sqrt{\rho^2\tilde{h}^2 - 2\mathcal{U}}}\left[q_4\frac{f_z}{\rho} + q_2\left(\rho^2\tilde{h}^2 - 2\mathcal{U}\right)\right], \tag{16}$$

$$\frac{\mathrm{d}q_2}{\mathrm{d}\phi} = \frac{1}{2\rho\tilde{h}\sqrt{\rho^2\tilde{h}^2 - 2\mathcal{U}}}\left[q_3\frac{f_z}{\rho} - q_1\left(\rho^2\tilde{h}^2 - 2\mathcal{U}\right)\right], \tag{17}$$

$$\frac{\mathrm{d}q_3}{\mathrm{d}\phi} = -\frac{1}{2\rho\tilde{h}\sqrt{\rho^2\tilde{h}^2 - 2\mathcal{U}}}\left[q_2\frac{f_z}{\rho} - q_4\left(\rho^2\tilde{h}^2 - 2\mathcal{U}\right)\right], \tag{18}$$

$$\frac{\mathrm{d}q_4}{\mathrm{d}\phi} = -\frac{1}{2\rho\tilde{h}\sqrt{\rho^2\tilde{h}^2 - 2\mathcal{U}}}\left[q_1\frac{f_z}{\rho} + q_3\left(\rho^2\tilde{h}^2 - 2\mathcal{U}\right)\right]. \tag{19}$$

2.2.3 Summary of the differential equations of motion

The time equation obtained by substituting Eq. (10) into Eq. (5):

$$\frac{\mathrm{d}t}{\mathrm{d}\phi} = \frac{1}{\rho^2\tilde{h}}, \tag{20}$$

together with Eqs. (11), (12) and Eqs. (16)–(19) represent a set of differential equations which govern the motion of the particle in terms of the eight state variables:

$$\left(t,\ \rho,\ \frac{\mathrm{d}\rho}{\mathrm{d}\phi},\ \tilde{h},\ q_1,\ q_2,\ q_3,\ q_4\right).$$

The above equations were also presented in a slight different form by Sharaf et al. (1992).

3 Generalized orbital elements

In this section we apply the variation of parameters technique to Eqs. (11) and (16)–(19) to derive the differential equations of seven generalized orbital elements. For convenience, we divide the orbital elements into two sets, the first defining the orbit shape while the second characterizing its orientation.

3.1 First set of elements

The only variable of the state vector that is already an integral of the unperturbed motion is the pseudo angular momentum $\tilde{h}$. Let us define the generalized orbital element ζ_3 as the inverse of $\tilde{h}$:

$$\zeta_3 = \frac{1}{\tilde{h}}. \tag{21}$$

In the case of pure Keplerian motion Eq. (11) reduces to:

$$\frac{\mathrm{d}^2\rho}{\mathrm{d}\phi^2} = -\rho + \zeta_3^2,$$

which can be solved analytically to yield:

$$\rho = \zeta_3 s, \tag{22}$$

$$\frac{\mathrm{d}\rho}{\mathrm{d}\phi} = -\zeta_3 u, \tag{23}$$

where:

$$s = \zeta_3 + \zeta_1 \cos\phi + \zeta_2 \sin\phi, \tag{24}$$

$$u = \zeta_1 \sin\phi - \zeta_2 \cos\phi, \tag{25}$$

and where ζ_1 and ζ_2 are two integration constants, which we will employ as generalized orbital elements.

First, let us rewrite the time equation (20) by exploiting Eqs. (21) and (22) as:

$$\frac{\mathrm{d}t}{\mathrm{d}\phi} = \frac{1}{\zeta_3 s^2}.$$

The differential equations of ζ_1, ζ_2 and ζ_3 are derived as follows. We substitute Eqs. (22) and (23) into Eq. (11), exploit Eq. (21) to substitute for $\tilde{h}$, and after simplifying and rearranging the terms, we get:

$$\frac{\mathrm{d}}{\mathrm{d}\phi}\left(\zeta_1(\phi)\sin\phi - \zeta_2(\phi)\cos\phi\right) = s - \zeta_3 + \frac{1}{s}\left(\frac{f_x}{\zeta_3 s} - 2\mathcal{U}\right). \tag{26}$$

Equation (26) and the osculating condition:

$$\frac{\mathrm{d}}{\mathrm{d}\phi}\left(\zeta_3(\phi)\left[\zeta_3(\phi) + \zeta_1(\phi)\cos\phi + \zeta_2(\phi)\sin\phi\right]\right) = -\zeta_3 u,$$

constitute a system of two algebraic equations which are solved for the derivatives of ζ_1 and ζ_2 with respect to ϕ to yield:

$$\frac{\mathrm{d}\zeta_1}{\mathrm{d}\phi} = \frac{\sin\phi}{s}\left(\frac{f_x}{\zeta_3 s} - 2\mathcal{U}\right) - \left(\frac{s}{\zeta_3} + 1\right)\cos\phi\,\frac{\mathrm{d}\zeta_3}{\mathrm{d}\phi},$$

$$\frac{\mathrm{d}\zeta_2}{\mathrm{d}\phi} = \frac{\cos\phi}{s}\left(2\mathcal{U} - \frac{f_x}{\zeta_3 s}\right) - \left(\frac{s}{\zeta_3} + 1\right)\sin\phi\,\frac{\mathrm{d}\zeta_3}{\mathrm{d}\phi},$$

where the derivative of the orbital element ζ_3 can be obtained by differentiation of Eq. (21) to finally find (for the algebraic details see Appendix II which is published as Electronic Supplementary Material):

$$\frac{\mathrm{d}\zeta_3}{\mathrm{d}\phi} = -\frac{1}{\tilde{h}^2}\frac{\mathrm{d}\tilde{h}}{\mathrm{d}\phi} = -\frac{1}{s^4}\left[u\zeta_3 s\left(2\mathcal{U} - \frac{\zeta_3 s}{s+\zeta_3}\frac{\partial\mathcal{U}}{\partial\zeta_3}\right) + P_y\sqrt{s^2 - 2\mathcal{U}} + \frac{\partial\mathcal{U}}{\partial t}\right].$$

3.2 Second set of elements

Equations (16)–(19) in purely Keplerian motion simplify to:

$$\frac{\mathrm{d}q_1}{\mathrm{d}\phi} = \frac{1}{2}q_2, \qquad \frac{\mathrm{d}q_2}{\mathrm{d}\phi} = -\frac{1}{2}q_1, \qquad \frac{\mathrm{d}q_3}{\mathrm{d}\phi} = \frac{1}{2}q_4, \qquad \frac{\mathrm{d}q_4}{\mathrm{d}\phi} = -\frac{1}{2}q_3.$$

These equations can be analytically integrated to give the solutions:

$$q_1 = \zeta_4 \cos\frac{\Delta\phi}{2} + \zeta_5 \sin\frac{\Delta\phi}{2}, \tag{27}$$

$$q_2 = \zeta_5 \cos\frac{\Delta\phi}{2} - \zeta_4 \sin\frac{\Delta\phi}{2}, \tag{28}$$

$$q_3 = \zeta_6 \cos\frac{\Delta\phi}{2} + \zeta_7 \sin\frac{\Delta\phi}{2}, \tag{29}$$

$$q_4 = \zeta_7 \cos\frac{\Delta\phi}{2} - \zeta_6 \sin\frac{\Delta\phi}{2}, \tag{30}$$

where $\Delta\phi = \phi - \phi_0$ and the four constants of integration $\zeta_4, \zeta_5, \zeta_6, \zeta_7$ represent the remaining generalized orbital elements.

By applying again the variation of parameters technique we substitute the solution (27)–(30) into Eqs. (16)–(19) and solve for the derivatives of $\zeta_4, \zeta_5, \zeta_6$ and ζ_7 with respect to ϕ to finally obtain:

$$\begin{aligned}
\frac{\mathrm{d}\zeta_4}{\mathrm{d}\phi} &= \frac{f_z}{2\zeta_3 s^2\sqrt{s^2-2\mathcal{U}}}\left(\zeta_7\cos\Delta\phi - \zeta_6\sin\Delta\phi\right) + \frac{\zeta_5}{2s}\left(\sqrt{s^2-2\mathcal{U}} - s\right),\\
\frac{\mathrm{d}\zeta_5}{\mathrm{d}\phi} &= \frac{f_z}{2\zeta_3 s^2\sqrt{s^2-2\mathcal{U}}}\left(\zeta_6\cos\Delta\phi + \zeta_7\sin\Delta\phi\right) - \frac{\zeta_4}{2s}\left(\sqrt{s^2-2\mathcal{U}} - s\right),\\
\frac{\mathrm{d}\zeta_6}{\mathrm{d}\phi} &= -\frac{f_z}{2\zeta_3 s^2\sqrt{s^2-2\mathcal{U}}}\left(\zeta_5\cos\Delta\phi - \zeta_4\sin\Delta\phi\right) + \frac{\zeta_7}{2s}\left(\sqrt{s^2-2\mathcal{U}} - s\right),\\
\frac{\mathrm{d}\zeta_7}{\mathrm{d}\phi} &= -\frac{f_z}{2\zeta_3 s^2\sqrt{s^2-2\mathcal{U}}}\left(\zeta_4\cos\Delta\phi + \zeta_5\sin\Delta\phi\right) - \frac{\zeta_6}{2s}\left(\sqrt{s^2-2\mathcal{U}} - s\right).
\end{aligned}$$

In Appendix II (published as Electronic Supplementary Material) the procedure to derive these four equations is outlined.

4 Summary of the differential equations of motion

The state variables that describe the motion of the particle around the primary are:

$$(t,\ \zeta_1,\ \zeta_2,\ \zeta_3,\ \zeta_4,\ \zeta_5,\ \zeta_6,\ \zeta_7), \tag{31}$$

and the corresponding differential equations with respect to the independent variable ϕ are:

$$\frac{\mathrm{d}t}{\mathrm{d}\phi} = \frac{1}{\zeta_3 s^2} \tag{32}$$

$$\frac{\mathrm{d}\zeta_1}{\mathrm{d}\phi} = \frac{\sin\phi}{s}\left(\frac{f_x}{\zeta_3 s} - 2\mathcal{U}\right) - \left(\frac{s}{\zeta_3} + 1\right)\cos\phi\,\frac{\mathrm{d}\zeta_3}{\mathrm{d}\phi} \tag{33}$$

$$\frac{\mathrm{d}\zeta_2}{\mathrm{d}\phi} = \frac{\cos\phi}{s}\left(2\mathcal{U} - \frac{f_x}{\zeta_3 s}\right) - \left(\frac{s}{\zeta_3} + 1\right)\sin\phi\,\frac{\mathrm{d}\zeta_3}{\mathrm{d}\phi} \tag{34}$$

$$\frac{\mathrm{d}\zeta_3}{\mathrm{d}\phi} = -\frac{1}{s^4}\left[u\zeta_3 s\left(2\mathcal{U} - \frac{\zeta_3 s}{s+\zeta_3}\frac{\partial \mathcal{U}}{\partial \zeta_3}\right) + \lambda P_y + \frac{\partial \mathcal{U}}{\partial t}\right] \tag{35}$$

$$\frac{\mathrm{d}\zeta_4}{\mathrm{d}\phi} = \frac{1}{2s}\left[\frac{f_z}{\zeta_3 s\lambda}\left(\zeta_7\cos\Delta\phi - \zeta_6\sin\Delta\phi\right) + \zeta_5\left(\lambda - s\right)\right] \tag{36}$$

$$\frac{\mathrm{d}\zeta_5}{\mathrm{d}\phi} = \frac{1}{2s}\left[\frac{f_z}{\zeta_3 s\lambda}\left(\zeta_6\cos\Delta\phi + \zeta_7\sin\Delta\phi\right) - \zeta_4\left(\lambda - s\right)\right] \tag{37}$$

$$\frac{\mathrm{d}\zeta_6}{\mathrm{d}\phi} = -\frac{1}{2s}\left[\frac{f_z}{\zeta_3 s\lambda}\left(\zeta_5\cos\Delta\phi - \zeta_4\sin\Delta\phi\right) - \zeta_7\left(\lambda - s\right)\right] \tag{38}$$

$$\frac{\mathrm{d}\zeta_7}{\mathrm{d}\phi} = -\frac{1}{2s}\left[\frac{f_z}{\zeta_3 s\lambda}\left(\zeta_4\cos\Delta\phi + \zeta_5\sin\Delta\phi\right) + \zeta_6\left(\lambda - s\right)\right], \tag{39}$$

where $\Delta\phi = \phi - \phi_0$, s and u are provided respectively by Eqs. (24) and (25):

$$s = \zeta_3 + \zeta_1\cos\phi + \zeta_2\sin\phi, \tag{40}$$

$$u = \zeta_1\sin\phi - \zeta_2\cos\phi, \tag{41}$$

and:

$$\lambda = \sqrt{s^2 - 2\mathcal{U}}. \tag{42}$$

It should be pointed out that the orbital element ζ_3 can be replaced by the total energy ε in the state vector. In this case we need the differential equation:

$$\frac{\mathrm{d}\varepsilon}{\mathrm{d}\phi} = \frac{1}{\zeta_3 s^2}\left(u P_x + P_y\sqrt{s^2 - 2\mathcal{U}} + \frac{\partial \mathcal{U}}{\partial t}\right),$$

which is derived in Appendix II (published as Electronic Supplementary Material). The quantity ζ_3 is computed from ε and the orbital elements ζ_1 and ζ_2 thanks to the relation:

$$\zeta_3 = \sqrt{\zeta_1^2 + \zeta_2^2 - 2\varepsilon},$$

which will be shown in Subsect. 5.4. As a rule of thumb, we say that the more conservative is the perturbation, the more advantageous in terms of accuracy and computational speed is the choice of ε in place of ζ_3 in the state vector. On the other hand, as we consider the case of a strongly non conservative perturbation, the computation of ζ_3 from ε, ζ_1 and ζ_2 is likely to produce a bigger error than numerically propagating ζ_3.

5 Collection of formulae for the implementation of the method

In this section will be developed useful relationships between the new generalized orbital elements and the Cartesian components of the position and velocity vectors expressed in a fixed reference frame and the classical orbital elements.

5.1 From the generalized orbital elements to the position and velocity vectors

First, we provide the relations to compute the components of the dimensionless position and velocity vectors expressed in a fixed reference frame $\mathcal{I}$:

$$\mathbf{r} = \left(R_X,\ R_Y,\ R_Z\right)^{\mathrm{T}}, \qquad \mathbf{v} = \left(V_X,\ V_Y,\ V_Z\right)^{\mathrm{T}},$$

from the generalized orbital elements $(\zeta_1, \ldots, \zeta_7)$.

Equations (22) and (23) are used along with Eqs. (10) and (5) to express the orbital radius r and the radial velocity v_r in function of $\zeta_1, \zeta_2, \zeta_3$ and ϕ as:

$$r = \frac{1}{\zeta_3 \left(\zeta_3 + \zeta_1 \cos\phi + \zeta_2 \sin\phi\right)}, \tag{43}$$

$$v_r = \zeta_1 \sin\phi - \zeta_2 \cos\phi. \tag{44}$$

Besides, the expression of the transverse velocity can be obtained as:

$$v_\theta = \frac{h}{r} = \sqrt{\left(\zeta_3 + \zeta_1 \cos\phi + \zeta_2 \sin\phi\right)^2 - 2\mathcal{U}}, \tag{45}$$

where we made use of Eqs. (6), (21) and (43). From comparison of Eqs. (44) and (45) with Eqs. (25) and (42) one infers that:

$$v_r = u, \qquad v_\theta = \lambda.$$

The position and velocity vectors of the particle can be expressed in $\mathcal{I}$ by the two matrix multiplications:

$$\left(R_X,\ R_Y,\ R_Z\right)^{\mathrm{T}} = Q_{\mathcal{RI}}\left(r,\ 0,\ 0\right)^{\mathrm{T}}, \tag{46}$$

$$\left(V_X,\ V_Y,\ V_Z\right)^{\mathrm{T}} = Q_{\mathcal{RI}}\left(u,\ \lambda,\ 0\right)^{\mathrm{T}}, \tag{47}$$

where $Q_{\mathcal{RI}}$ is the rotation matrix between the local-vertical local-horizontal frame $\mathcal{R}$ and the fixed frame $\mathcal{I}$ and will be computed as follows.

The relations (27)–(30) correspond to a quaternion product:

$$\hat{q} = \hat{\zeta}\hat{z}, \tag{48}$$

where $\hat{q}$ was defined by Eqs. (14) and (15), and we have introduced the two unit quaternions:

$$\hat{\zeta} = \left(\zeta_7,\ \boldsymbol{\zeta}\right), \qquad \hat{z} = \left(\cos\frac{\triangle\phi}{2},\ \mathbf{z}\right),$$

with the vectorial part given by:

$$\boldsymbol{\zeta} = \left(\zeta_4,\ \zeta_5,\ \zeta_6\right), \qquad \mathbf{z} = \left(0,\ 0,\ \sin\frac{\triangle\phi}{2}\right).$$

The unit quaternion $\hat{q}$, as seen in Subsect. 2.2, is associated to the rotation matrix $Q_{\mathcal{RI}}$, while the corresponding rotation matrices for $\hat{\zeta}$ and $\hat{z}$ are, respectively:

$$Q_0 = \begin{bmatrix} 1-2\zeta_5^2-2\zeta_6^2 & 2\zeta_4\zeta_5-2\zeta_6\zeta_7 & 2\zeta_4\zeta_6+2\zeta_5\zeta_7 \\ 2\zeta_4\zeta_5+2\zeta_6\zeta_7 & 1-2\zeta_4^2-2\zeta_6^2 & 2\zeta_5\zeta_6-2\zeta_4\zeta_7 \\ 2\zeta_4\zeta_6-2\zeta_5\zeta_7 & 2\zeta_5\zeta_6+2\zeta_4\zeta_7 & 1-2\zeta_4^2-2\zeta_5^2 \end{bmatrix}, \tag{49}$$

$$M_\phi = \begin{bmatrix} \cos\triangle\phi & -\sin\triangle\phi & 0 \\ \sin\triangle\phi & \cos\triangle\phi & 0 \\ 0 & 0 & 1 \end{bmatrix}. \tag{50}$$

The relation between $Q_{\mathcal{RI}}$, Q_0 and M_ϕ, analogous to the product (48), is the matrix multiplication:

$$Q_{\mathcal{RI}} = Q_0 M_\phi. \tag{51}$$

After performing the products in Eqs. (46) and (47), where the matrix $Q_{\mathcal{RI}}$ is determined according to Eq. (51) by employing Eqs. (49) and (50), we obtain the six components:

$$
\begin{aligned}
R_X &= r\left[(1-2\zeta_5^2-2\zeta_6^2)\cos\Delta\phi + 2\,(\zeta_4\zeta_5-\zeta_6\zeta_7)\sin\Delta\phi\right],\\
R_Y &= r\left[(1-2\zeta_4^2-2\zeta_6^2)\sin\Delta\phi + 2\,(\zeta_4\zeta_5+\zeta_6\zeta_7)\cos\Delta\phi\right],\\
R_Z &= 2r\left[(\zeta_5\zeta_6+\zeta_4\zeta_7)\sin\Delta\phi + (\zeta_4\zeta_6-\zeta_5\zeta_7)\cos\Delta\phi\right],\\
V_X &= \left[2\lambda\,(\zeta_4\zeta_5-\zeta_6\zeta_7)+u(1-2\zeta_5^2-2\zeta_6^2)\right]\cos\Delta\phi\\
&\quad+\left[2u\,(\zeta_4\zeta_5-\zeta_6\zeta_7)-\lambda(1-2\zeta_5^2-2\zeta_6^2)\right]\sin\Delta\phi,\\
V_Y &= \left[\lambda(1-2\zeta_4^2-2\zeta_6^2)+2u\,(\zeta_4\zeta_5+\zeta_6\zeta_7)\right]\cos\Delta\phi\\
&\quad+\left[u(1-2\zeta_4^2-2\zeta_6^2)-2\lambda\,(\zeta_4\zeta_5+\zeta_6\zeta_7)\right]\sin\Delta\phi,\\
V_Z &= 2\left[\lambda\,(\zeta_5\zeta_6+\zeta_4\zeta_7)+u\,(\zeta_4\zeta_6-\zeta_5\zeta_7)\right]\cos\Delta\phi\\
&\quad+2\left[u\,(\zeta_5\zeta_6+\zeta_4\zeta_7)-\lambda\,(\zeta_4\zeta_6-\zeta_5\zeta_7)\right]\sin\Delta\phi.
\end{aligned}
$$

5.2 From the position and velocity vectors to the generalized orbital elements

In the following we show how to compute the generalized orbital elements $(\zeta_1,\ldots\zeta_7)$ from the components of the position and velocity vectors expressed in the fixed frame $\mathcal{I}$, that is $(R_X,\ R_Y,\ R_Z)$ and $(V_X,\ V_Y,\ V_Z)$.

By solving Eqs. (43), (44) and (45) for the three orbital elements ζ_1, ζ_2 and ζ_3, one derives the relations:

$$\zeta_1 = \left(\sqrt{\lambda^2+2\mathcal{U}}-\frac{1}{r\sqrt{\lambda^2+2\mathcal{U}}}\right)\cos\phi + u\sin\phi, \tag{52}$$

$$\zeta_2 = \left(\sqrt{\lambda^2+2\mathcal{U}}-\frac{1}{r\sqrt{\lambda^2+2\mathcal{U}}}\right)\sin\phi - u\cos\phi, \tag{53}$$

$$\zeta_3 = \frac{1}{r\sqrt{\lambda^2+2\mathcal{U}}}, \tag{54}$$

where

$$
\begin{aligned}
r &= \sqrt{R_X^2+R_Y^2+R_Z^2},\\
u &= \mathbf{v}\cdot\mathbf{i} = \frac{R_XV_X+R_YV_Y+R_ZV_Z}{r},\\
\lambda &= \mathbf{v}\cdot\mathbf{j} = \frac{h}{r},
\end{aligned}
$$

with

$$
\begin{aligned}
h &= \sqrt{H_X^2+H_Y^2+H_Z^2},\\
H_X &= R_YV_Z-R_ZV_Y, \qquad H_Y = R_ZV_X-R_XV_Z, \qquad H_Z = R_XV_Y-R_YV_X.
\end{aligned}
$$

The relations of the remaining orbital elements can be derived from Eq. (49):

$$\zeta_4 = \frac{Q_0\,(3,2)-Q_0\,(2,3)}{4\zeta_7}, \tag{55}$$

$$\zeta_5 = \frac{Q_0\,(1,3)-Q_0\,(3,1)}{4\zeta_7}, \tag{56}$$

$$\zeta_6 = \frac{Q_0(2,1) - Q_0(1,2)}{4\zeta_7}, \tag{57}$$

$$\zeta_7 = \pm\frac{1}{2}\sqrt{1 + Q_0(1,1) + Q_0(2,2) + Q_0(3,3)}, \tag{58}$$

with (Eq. 51):

$$Q_0 = Q_{\mathcal{RI}} M_\phi^{\mathrm{T}}, \tag{59}$$

where M_ϕ is given in Eq. (50) and $Q_{\mathcal{RI}}$ can be written by columns as:

$$Q_{\mathcal{RI}} = \left(\frac{\mathbf{r}}{r}, \frac{\mathbf{r}\times\mathbf{v}}{|\mathbf{r}\times\mathbf{v}|} \times \frac{\mathbf{r}}{r}, \frac{\mathbf{r}\times\mathbf{v}}{|\mathbf{r}\times\mathbf{v}|}\right).$$

By substituting into Eqs. (55)–(58) the elements of the matrix Q_0 as derived in Appendix I we finally have:

$$\zeta_4 = \frac{1}{4\zeta_7}\left[\left(\frac{H_X R_Y - H_Y R_X}{rh}\right)\cos\Delta\phi + \frac{R_Z}{r}\sin\Delta\phi - \frac{H_Y}{h}\right],$$

$$\zeta_5 = \frac{1}{4\zeta_7}\left[\left(\frac{H_X R_Y - H_Y R_X}{rh}\right)\sin\Delta\phi - \frac{R_Z}{r}\cos\Delta\phi + \frac{H_X}{h}\right],$$

$$\zeta_6 = \frac{1}{4\zeta_7}\left[\left(\frac{H_X R_Z - H_Z R_X}{rh} - \frac{R_X}{r}\right)\sin\Delta\phi + \left(\frac{H_Z R_Y - H_Y R_Z}{rh} + \frac{R_Y}{r}\right)\cos\Delta\phi\right],$$

$$\zeta_7 = \pm\frac{1}{2}\sqrt{1 + \frac{H_Z}{h} + \left(\frac{H_Z R_X - H_X R_Z}{rh} + \frac{R_X}{r}\right)\cos\Delta\phi + \left(\frac{H_Z R_Y - H_Y R_Z}{rh} + \frac{R_Y}{r}\right)\sin\Delta\phi}.$$

The singular case $\zeta_7 = 0$ is discussed in the Appendix I.

5.3 From the classical to the generalized orbital elements

We provide the relations to compute the generalized orbital elements $(\zeta_1, \ldots, \zeta_7)$ from the classical orbital elements:

$$(h,\ e,\ \nu,\ i,\ \Omega,\ \omega),$$

with h the dimensionless angular momentum, e the eccentricity, ν the true anomaly, i the inclination, Ω the longitude of the ascending node and ω the argument of pericenter.

The orbital radius r, radial velocity u, and transverse velocity λ can be written as (see for instance at pages 117 and 126 of Battin 1999):

$$r = \frac{h^2}{1 + e\cos\nu}, \tag{60}$$

$$u = \frac{1}{h} e\sin\nu, \tag{61}$$

$$\lambda = \frac{1}{h}(1 + e\cos\nu). \tag{62}$$

By inserting these expressions into Eqs. (52)–(54), after some algebra we have:

$$\zeta_1 = \left[\frac{e\cos\nu\,(1+e\cos\nu)+2\mathcal{U}h^2}{h\sqrt{(1+e\cos\nu)^2+2\mathcal{U}h^2}}\right]\cos\phi+\frac{e}{h}\sin\nu\sin\phi,$$
$$\zeta_2 = \left[\frac{e\cos\nu\,(1+e\cos\nu)+2\mathcal{U}h^2}{h\sqrt{(1+e\cos\nu)^2+2\mathcal{U}h^2}}\right]\sin\phi-\frac{e}{h}\sin\nu\cos\phi,$$
$$\zeta_3 = \frac{1+e\cos\nu}{h\sqrt{(1+e\cos\nu)^2+2\mathcal{U}h^2}}.$$

The four Euler parameters ζ_4, ζ_5, ζ_6, and ζ_7 are associated to the Euler angle sequence $(\Omega,\ i,\ \omega+\nu-\triangle\phi)$, as we infer from Eq. (59). As a consequence, the following relations can be established:

$$\zeta_4 = \sin\frac{i}{2}\cos\frac{\Omega-\omega-\nu+\triangle\phi}{2},$$
$$\zeta_5 = \sin\frac{i}{2}\sin\frac{\Omega-\omega-\nu+\triangle\phi}{2},$$
$$\zeta_6 = \cos\frac{i}{2}\sin\frac{\Omega+\omega+\nu-\triangle\phi}{2},$$
$$\zeta_7 = \cos\frac{i}{2}\cos\frac{\Omega+\omega+\nu-\triangle\phi}{2}.$$

5.4 From the generalized to the classical orbital elements

We derive the relations to compute the classical orbital elements $(h,\ e,\ \nu,\ i,\ \Omega,\ \omega)$ from the generalized orbital elements $(\zeta_1,\ldots,\zeta_7)$.

First, by using Eqs. (43)–(45) to substitute for r, u and λ on the left-hand side of Eqs. (60)–(62), and then solving for the dimensionless angular momentum h, eccentricity e and true anomaly ν, we derive:

$$h = \frac{\sqrt{s^2-2\mathcal{U}}}{\zeta_3 s},$$
$$e = \frac{1}{\zeta_3 s}\sqrt{\left(s^2-2\mathcal{U}\right)\left(\zeta_1^2+\zeta_2^2-2\mathcal{U}\right)+2\mathcal{U}\zeta_3^2},$$
$$\nu = \tan^{-1}\left(\frac{u\sqrt{s^2-2\mathcal{U}}}{s^2-2\mathcal{U}-\zeta_3 s}\right).$$

The expressions of the inclination i, longitude of the ascending node Ω and argument of pericenter ω are obtained by equating the components of the matrix Q_0 expressed in terms of quaternions (Eq. 49) and described by the Euler angle sequence $(\Omega,\ i,\ \omega+\nu-\triangle\phi)$ as can be inferred from Eq. (59):

$$i = \cos^{-1}\left(1-2\zeta_4^2-2\zeta_5^2\right),$$
$$\Omega = \tan^{-1}\left(\frac{\zeta_4\zeta_6+\zeta_5\zeta_7}{\zeta_4\zeta_7-\zeta_5\zeta_6}\right),$$
$$\omega = \triangle\phi-\nu+\tan^{-1}\left(\frac{\zeta_4\zeta_6-\zeta_5\zeta_7}{\zeta_5\zeta_6+\zeta_4\zeta_7}\right).$$

Finally, the total energy ε can be computed directly from ζ_1, ζ_2 and ζ_3 by exploiting Eqs. (21), (43) and (44):

$$\varepsilon = \frac{1}{2}\left(v_r^2 + \frac{\tilde{h}^2}{r^2}\right) - \frac{1}{r} = \frac{\zeta_1^2 + \zeta_2^2 - \zeta_3^2}{2}.$$

6 Disturbing potential

When introducing the generalized Sundman time transformation defined by Eqs. (5) and (6) the following constraint has to be satisfied in order to guarantee the existence of $\tilde{h}$ and avoid singularities:

$$\mathcal{U} > -\frac{v_\theta^2}{2}. \tag{63}$$

As far as the characterization of the function $\mathcal{U}$ the main conservative perturbation relevant to astrodynamical problem is of gravitational origin and can stem from higher spherical harmonics of the primary body as well as from the gravitational disturbance of third bodies. In the first case it is possible to prove that the above condition can only be violated when the particle is located inside the primary physical envelope. The second case is more complicated to evaluate and violations of Eq. (63) can occur. On the other hand this fact is not of concern as an arbitrary constant can always be added to $\mathcal{U}$ to remove the singularity (as both the disturbing potential energy and the particle transversal velocity are bounded under realistic conditions). Moreover, the third body perturbation is almost always expressed directly as a force obtained through accurate ephemeris data and rarely considered in potential form.

In the case in which the acting perturbations are not derivable from a potential, or are not considered as such, the function $\mathcal{U}$ can still be used as a pure constant to eliminate the singularity affecting Peláez's method for vanishing transversal velocity ($h = 0$ in Eq. 2). For the purpose of eliminating the singularity any positive constant value for $\mathcal{U}$ can be chosen, as it is evident from Eq. (63). However, some care should be taken in this regard as the chosen value may affect the performance of the method [2].

7 Performance of the method

In this section we test the performance of our method by adopting some known examples in the literature. The aim is twofold: to show the appreciable gain in performance with respect to Peláez's special perturbation method (Peláez et al. 2007), and to compare our formulation with other very efficient element methods coming from the Kustaanheimo-Stiefel and the Sperling-Burdet regularizations.

Because all the propagation methods considered here involve first-order ordinary differential equations it is reasonable to choose the same numerical integrator. Accordingly, an appropriate and reliable performance parameter is the number of *function calls*, that is the total number of evaluations of the derivative of the state vector with respect to the fictitious time. Referring to the number of function calls makes our analysis completely independent of uncontrolled factors related to the particular environment where the simulations are run.

[2] Note for instance that setting $\mathcal{U} \neq 0$ the resulting dependent variables $(\zeta_1, \ldots, \zeta_7)$ are not constant in the unperturbed motion.

The comparison is done by monitoring the number of function calls and the achieved accuracy of each method by varying the relative tolerance of the numerical integrator. Basically, we can say that the best method shows the lowest function evaluations for a required level of accuracy, or equivalently, the best accuracy for a given number of function calls. We also provide plots that show the error of the position and physical time as a function of the normalized independent variable which is defined by the ratio:

$$\chi = \frac{\tau}{\max(\tau)}, \tag{64}$$

where τ is the time-like argument of a certain method.

The following propagation schemes are compared: the method proposed in this paper, Peláez's special perturbation method (Peláez et al. 2007), the Sperling-Burdet's set of spatial and temporal elements as presented in Chapter 9 of Bond and Allman (1996), and the Stiefel-Scheifele's set of elements as described in Section 19 of Stiefel and Scheifele (1971). The latter was considered also by Arakida and Fukushima (2001) in a comparison of the performance of different element methods generated by the K-S regularization. Note that only the last two methods employ a complete set of elements because a time-element (Stiefel and Scheifele 1971, Section 18) is used in place of the physical time in the state vector. On the other hand, both our formulation and the Dromo method do not take advantage of a time-element [3] and the physical time is a dependent variable. Therefore, for the fairness of comparison we decided to replace in the state vector of the Sperling-Burdet and Stiefel-Scheifele formulations the time-element with the physical time.

The propagators were implemented in the Matlab environment (version 2009a), and the explicit Runge-Kutta (4, 5) pair of Dormand and Prince (DP54, see Section II.5 of Hairer et al. 2009), which is provided by the ode45 function of Matlab, was selected as the numerical integrator.

We report and discuss below the performance diagrams for some typical problems in astrodynamics.

7.1 Problem description and performance analysis

Let us consider a spacecraft around the Earth. The components of the position vector of the spacecraft at the initial epoch projected into an Earth-centered inertial frame $\mathcal{I}$ are reported in Table 1. The velocity vector at the initial epoch is oriented along the X positive direction and its magnitude depends on the selected eccentricity of the initial osculating orbit. This orbit has an inclination of nearly 30° and the spacecraft is at the perigee at an orbital distance of 6800 km. Table 1 reports the velocity vector at the initial epoch for an eccentricity of 0.95, which represents the case considered in Section 23 of Stiefel and Scheifele (1971).

The motion is propagated up to the desired epoch in three different perturbed scenarios involving the Earth's oblateness, the Moon's third body gravitational attraction and the Earth's atmospheric drag. The accuracy of each method is assessed by computing the error that affects the spacecraft position vector at the end of the numerical propagation. Let X_e, Y_e, and Z_e be the components of the exact position at some epoch, and X_a, Y_a, and Z_a the approximated position obtained from one of the compared methods, then the error is calculated as:

$$\delta = \sqrt{(X_e - X_a)^2 + (Y_e - Y_a)^2 + (Z_e - Z_a)^2}.$$

[3] The possibility of introducing a time-element in our set of elements will be presented in a forthcoming paper.

Table 1 Initial position and velocity vectors expressed in an Earth-centered inertial frame as employed in Stiefel and Scheifele (1971)

$R_{X,0}$ (km)	$R_{Y,0}$ (km)	$R_{Z,0}$ (km)	$V_{X,0}$ (km/s)	$V_{Y,0}$ (km/s)	$V_{Z,0}$ (km/s)
0	−5888.9727	−3400	10.691338	0	0

The resulting Keplerian orbit is a highly eccentric ellipse (the eccentricity is 0.95) and has an inclination of nearly 30°

Because an analytical solution will not be available a *reference solution* for the position vector is derived with the following procedure: after running the four compared schemes by setting a tight relative tolerance of the numerical integrator, we keep the common figures in each component of the final position vector.

The time range of propagation is chosen in order to allow a number of revolutions that is sufficiently high for accumulating an appreciable error, and to stop the spacecraft when it is the furthest possible from the Earth because the slower dynamics improves the accuracy of the reference solution.

As regards the computation of the error during the numerical integration the same procedure described by Fukushima in (2007b) is followed. Two propagations are carried out with a Runge-Kutta of order four (RK4): the first uses a step size h and the second a halved step size $h/2$. Then, an accurate estimate of the position and physical time errors is given by:

$$\triangle \mathbf{r} = \frac{16}{15}\left[(\mathbf{r}_h - \mathbf{r}_{h/2}) - \mathbf{v}_{h/2}(t_h - t_{h/2})\right], \tag{65}$$

$$\triangle t = \frac{16}{15}(t_h - t_{h/2}), \tag{66}$$

where the subscript indicates the step size. Note that the position error $\triangle \mathbf{r}$ is referred to the physical time t_h which, in general, is different from $t_{h/2}$.

For convenience we will use the following labels to refer to the methods in the performance diagrams and, when necessary, in the text: "Dromo(P)" for the method presented in this paper, "Dromo" for Peláez's special perturbation method, "Spe&Bur" and "Sti&Sche" for the Sperling-Burdet and Stiefel-Scheifele formulations respectively both with the physical time employed in place of the time-element.

7.1.1 Earth's oblateness

A spacecraft, with initial conditions provided in Table 1, is perturbed by the second zonal harmonic of the Earth's gravity field which represents the equatorial bulge. The corresponding perturbing potential energy is given by (Battin 1999, p. 503):

$$\mathcal{U} = \frac{\mu_E R_E^2 J_2}{2r^3}\left(3\cos^2\theta - 1\right), \tag{67}$$

where the orbital radius r is meant as dimensional here, θ is the colatitude and the Earth's radius R_E, gravitational parameter μ_E and oblateness coefficient J_2 take the values:

$$R_E = 6371.22\,\text{km}, \qquad \mu_E = 398601\,\text{km}^3/\text{s}^2, \qquad J_2 = 1.08265 \times 10^{-3}.$$

The motion is propagated up to 289.66457509 mean solar days (msd) from the initial epoch, when the spacecraft has completed 49.5 revolutions around the Earth. This problem is the same presented in the "Example 1" at page 119 of Stiefel and Scheifele (1971).

Table 2 Reference position vector at the final time expressed in an Earth-centered inertial frame

Examples	X_e (km)	Y_e (km)	Z_e (km)
J_2	−19330.6793	228708.2356	130258.6070
J_2+Moon			
$e = 0.95$	−24219.0501	227962.10637	129753.44240
$e = 0.7$	−3529.0232	33375.887010	18838.29677
$e = 0.3$	−1142.351295	11002.0634065	6042.183235
$e = 0$	−587.059481	6017.7665435	3094.323699
J_2 + drag	3754.122945	−5623.63869	708.40001

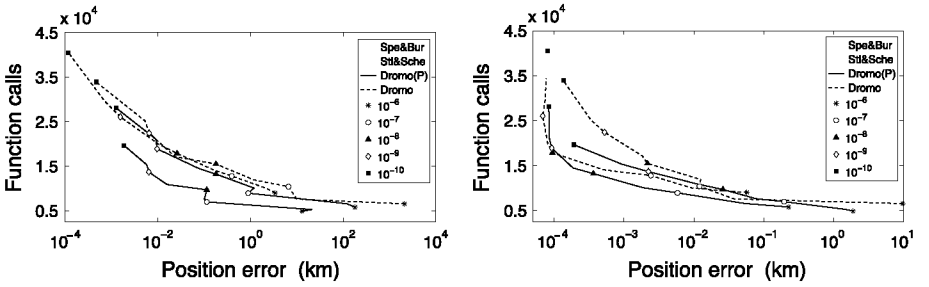

Fig. 1 Number of function calls of the DP54 integrator versus position error with J_2 perturbation. The propagation starts from an ellipse of eccentricity 0.95 and (*left*) stops after 49.5 revolutions (289.66457509 msd). The plot on the *right* shows the same performance diagram when an accurate propagation of the physical time is performed. The markers refer to different values of the relative tolerance of the numerical integrator

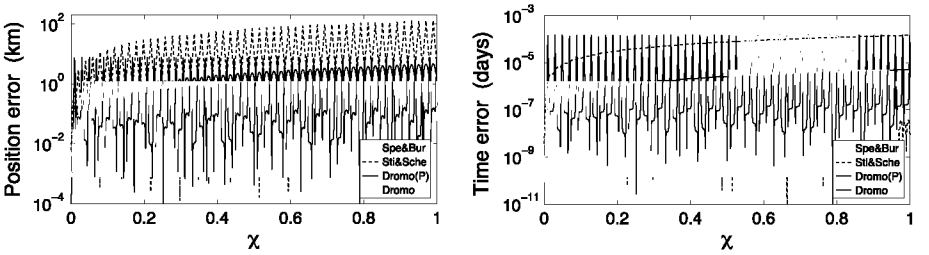

Fig. 2 Magnitude (*left*) of the position vector error (Eq. 65) and (*right*) of the time error (Eq. 66) versus normalized time-like argument (Eq. 64) for the same problem of Fig. 1. The motion is propagated by the RK4 integrator with 3168 steps (64 steps per revolution)

The reference position at the final epoch is reported in the first row of Table 2. In Fig. 1, left, the performance of the methods are compared. Dromo(P) requires fewer function calls than Dromo for a given error, or equivalently is more accurate for the same number of function calls. Moreover, it is notable that the maximum error is nearly one order of magnitude smaller for Dromo(P) than Dromo. A deeper analysis has revealed that the main source of error for the position is due to the error affecting the physical time which has a dominant effect over the error of the orbital elements employed by each method. The influence of the latter on the position error can be assessed as follows.

For each formulation the same final value of the independent variable is set to stop the numerical integrations with different relative tolerances of the integrator. This value of the independent variable is determined in such a way that when it is used to stop a propagation

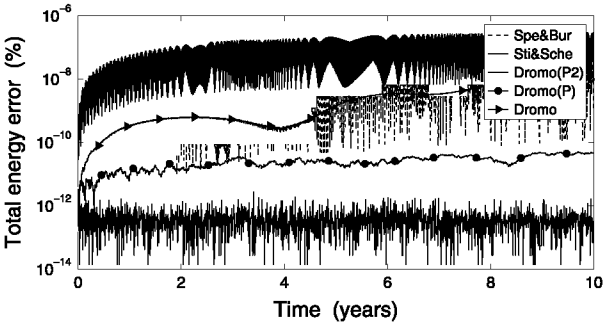

Fig. 3 Total energy error (Eq. 68) for a long-term propagation of 10 years under J_2 perturbation and starting from an ellipse of eccentricity 0.95

which is performed with the tightest relative tolerance available (we choose 10^{-13} for the integrator DP54) then the physical time at the end of the numerical integration is *exactly* (the error is at the rounding-off level) the desired final time of propagation. However when the accurate final independent variable is employed with a different (higher) value of the relative tolerance the physical time differs from the desired time of propagation by some variable amount for each method. Figure 1, right, shows the error of the position which has been obtained in this way. Dromo(P) not only considerably improves Dromo but also exhibits the best performance. This fact suggests that the implementation of a time-element in Dromo(P), at least for the problem under consideration, may greatly increase the efficiency of the method.

The error accumulation of the position and physical time with respect to the normalized time-like argument χ defined in Eq. (64) is shown in Fig. 2, left, and 2, right, respectively. Peaks of similar amplitude for Dromo(P) and Dromo characterize the error near the apogee. While the amplitude of these peaks does not increase, the mean error grows linearly between two consecutive apogees but with a smaller slope for Dromo(P) than Dromo so that our proposed method seems to be more suited to long-term propagations.

Finally, because the perturbation is derivable from a conservative potential the total energy is constant and equal to the value ε_0 of the initial epoch. For this reason it is interesting to compute the total energy ε from the spacecraft position and velocity vectors and check the variation of the relative error:

$$\xi = \frac{|\varepsilon - \varepsilon_0|}{\varepsilon_0}. \tag{68}$$

Figure 3 plots this error in function of the physical time for a long-term integration. In the comparison we include also the formulation of our method where the state variable ζ_3 is replaced by the total energy ε, and we refer to this variation of Dromo(P) as Dromo(P2). As we said in Sect. 4 the employment of the total energy is advantageous especially when the perturbations are conservative. The curves were obtained by setting a tight relative tolerance (10^{-12}) of the numerical integrator. Dromo(P2) along with Dromo(P) show the best behavior and the error does not increase for Dromo(P2).

7.1.2 Earth's oblateness and Moon's third body gravitational attraction

We refer now to the "Example 2" at page 121 of Stiefel and Scheifele (1971). This example has been used for comparing the performance of different methods also by Bond (1974), in Section 9.7 of Bond and Allman (1996) and by Peláez et al. (2007). The motion is perturbed by the Earth's oblateness, which, like in the previous example, is introduced as the J_2 perturbing

potential energy in Eq. (67), and by the Moon's attraction, which instead is implemented as a perturbing force. The orbit of the Moon is assumed circular and its position vector in the Earth-centered inertial frame is:

$$X_M = \varrho \sin\left(w\bar{t}\right), \qquad Y_M = -\frac{\sqrt{3}}{2}\varrho \cos\left(w\bar{t}\right), \qquad Z_M = -\frac{1}{2}\varrho \cos\left(w\bar{t}\right),$$

where $\bar{t}$ is the physical time. Moon's orbital radius, angular velocity and gravitational parameter take the values:

$$\varrho = 384400\,\mathrm{km}, \qquad w = 2.665315780887 \times 10^{-6}\,\mathrm{s}^{-1}, \qquad \mu_M = 4902.66\,\mathrm{km}^3/\mathrm{s}^2.$$

We first selected the initial position and velocity provided in Table 1, and the motion was propagated through 288.12768941 msd, which is the same time interval chosen in the "Example 2b" at page 122 of Stiefel and Scheifele (1971). Then, the initial X-component of the velocity in Table 1 was gradually decreased in order to lower the apogee radius, while keeping unchanged the perigee radius and the other classical orbital elements. More specifically, the additional initial eccentricities 0.7, 0.3 and 0 were chosen. The time of propagation is set for each case to allow 49.5 revolutions around the Earth and the reference positions are found in Table 2. Figure 4 collects the four performance diagrams for the considered initial conditions. The results reveal the eccentricity dependence of the position error of Dromo(P) in the sense that we now explain. By lowering the apogee altitude the motion takes place nearer to the Earth and farther from the Moon, therefore the Earth's oblateness becomes the main perturbation for an increasingly large time of propagation. When the initial eccentricity is 0 the Moon's attraction is negligible and the spacecraft is always perturbed by a strong nearly conservative force field. For this reason Dromo(P) behaves better for small eccentricities than Dromo and it is worth noting that for the case of initial circular orbit it ranks first among the compared methods.

Let us focus on the 0 and 0.3 initial eccentricity examples, and investigate the accumulation of the position and time error during the numerical integration. Figure 5 contains the plots of such errors which are computed by Eqs. (65) and (66). For near-circular motion only Dromo(P) and the Sperling-Burdet method enjoy the linear dependence of the error averaged over one revolution for both position and time, while the average errors produced by Dromo and the Stiefel-Scheifele method follow the quadratic law $a\tau^2+b\tau$, where τ is the independent variable and the coefficients a and b can be conveniently computed. For moderate eccentricity linearity characterizes the average error growth of the physical time of all methods and in particular we note that the rate of accumulation is smaller of a factor around 30 for Dromo(P) than for Dromo. As concerns the position error two different trends of accumulation appear both in Dromo and Dromo(P), with the latter showing a much better performance than the former.

One final remark is on the fact that by decreasing the eccentricity the Stiefel-Scheifele method progressively loses accuracy while Dromo(P) improves its performance. In fact it is significant that for the case of zero initial eccentricity the level of accuracy reached by Sti&Sche with the tightest relative tolerance (10^{-10}) is still worse than Dromo(P) with a relative tolerance of 10^{-6}.

7.1.3 Earth's oblateness and atmospheric drag

We finally address an example involving the atmospheric drag which produces a force not derivable from a potential. An object of mass m acted upon by the atmospheric drag force undergoes the acceleration (Vallado 2001, p. 525):

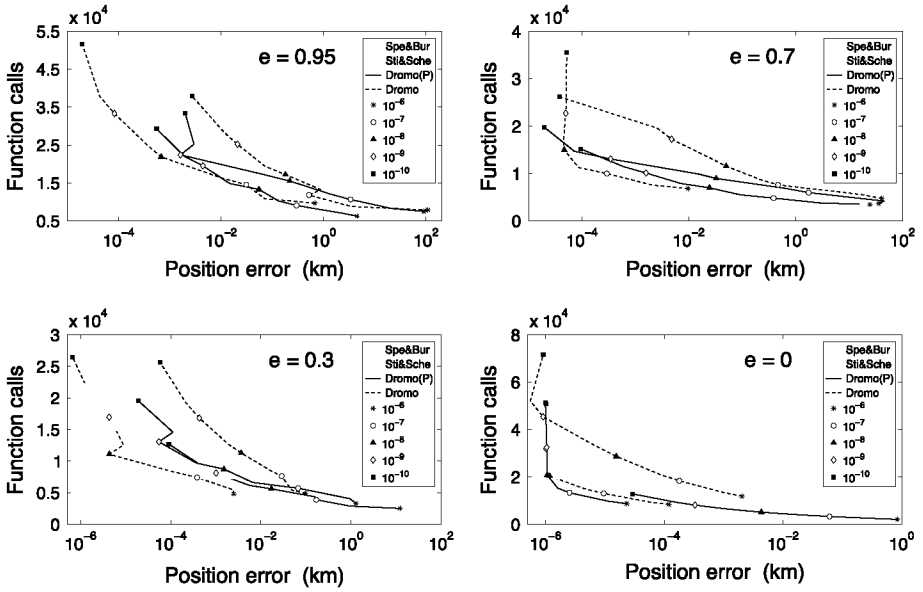

Fig. 4 Number of function calls of the DP54 integrator versus position error under J_2 and Moon's attraction perturbations for 49.5 revolutions and with different eccentricities e of the initial osculating orbit. The time propagation is 288.12768941 msd for $e = 0.95$, 19.43348169 msd for $e = 0.7$, 5.45405849 msd for $e = 0.3$, and 3.19412898 msd for $e = 0$. The markers refer to different values of the relative tolerance of the numerical integrator

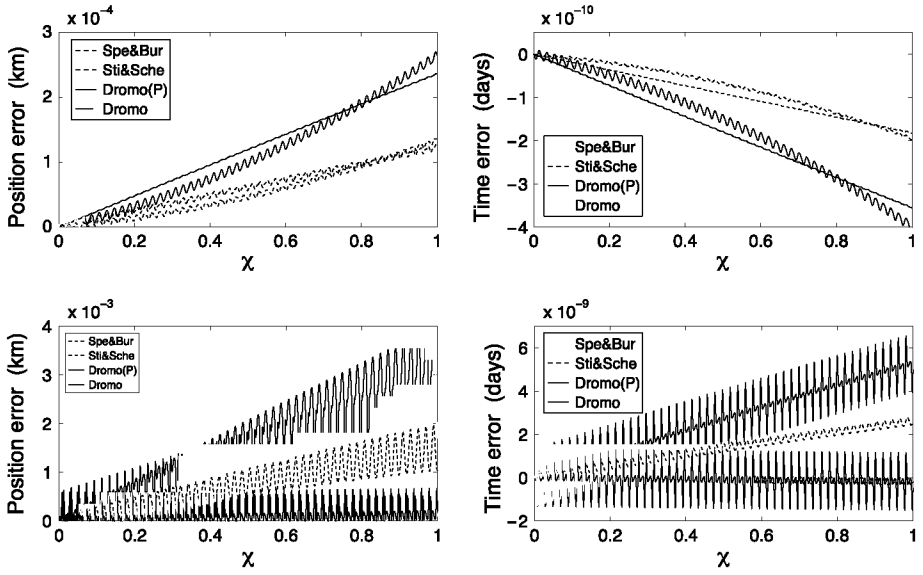

Fig. 5 Magnitude (*left column*) of the position vector error (Eq. 65) and (*right column*) time error (Eq. 66) versus normalized time-like argument (Eq. 64) with J_2 and Moon's attraction perturbations. The motion is propagated from a circular orbit (*upper row*) and an ellipse of eccentricity 0.3 (*lower row*) through 49.5 revolutions by the RK4 integrator with 3168 steps (64 steps per revolution)

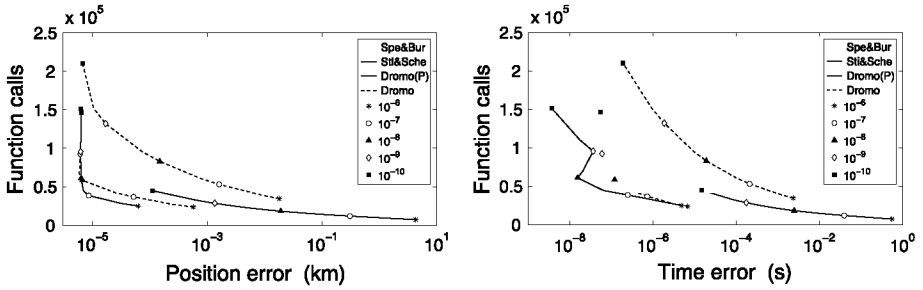

Fig. 6 Number of function calls of the DP54 integrator versus (*left*) position error and (*right*) time error with J_2 and drag perturbations. The propagation starts from a circular orbit and stops after 150 revolutions. The markers refer to different values of the relative tolerance of the numerical integrator

$$\mathbf{P} = -\frac{1}{2}\rho C_D \frac{A}{m} v_{rel} \mathbf{v}_{rel},$$

where we set for the drag coefficient and the surface to mass ratio the following values typical of a compact spacecraft in free molecular flow:

$$C_D = 2.2, \qquad \frac{A}{m} = 0.01 \frac{\mathrm{m}^2}{\mathrm{kg}}.$$

The velocity of the atmosphere at the spacecraft location, which is required to compute the relative velocity vector $\mathbf{v}_{rel}$, is written in an Earth-centered inertial frame as:

$$\mathbf{v}_{atm} = w_E \, (-R_Y, \, R_X, \, 0)^{\mathrm{T}},$$

where $w_E = 7.29211585531 \times 10^{-5}$ rad/s is the angular speed of the Earth's rotation and the components R_X and R_Y define the spacecraft position projected in the equatorial plane. The exponential atmospheric model is employed to determine the atmosphere density ρ according to the relation (Vallado 2001, p. 535):

$$\rho = \rho_0 \exp\left(-\frac{h - h_0}{H}\right),$$

where the height above the Earth's surface is calculated as the difference between the orbital distance and the Earth's radius $h = r - R_E$, and the base altitude h_0, the scale height H and the nominal density ρ_0 are taken from Table 8.4 at page 537 of Vallado (2001).

The second perturbation that is considered apart from drag is the J_2 zonal harmonic, which as in the previous examples is introduced by means of the potential energy in Eq. (67). The propagation starts from a circular orbit (the initial conditions are the same of the example with $e = 0$ in the previous subsection) and continues through a suitable number of revolutions (namely 150) for appreciating the effect of drag on the trajectory. The reference position vector is contained in the last row of Table 2. Figure 6, left, shows that Dromo(P) is the most accurate method for a given number of function calls while Dromo is the worst in this sense. The considerable gain in performance which is achieved by Dromo(P) with respect to Dromo is mainly due to the strong reduction of the numerical integration error affecting the physical time as can be appreciated in Fig. 6, right, Such figure is obtained similarly to Fig. 1, right, by employing with a certain method the same accurate final value of the independent variable for all the chosen relative tolerances. The dependence of the position and time errors on the time-like argument is the same observed in Fig. 5, upper row, where Dromo(P) and Dromo exhibit a linear and quadratic character of the error growth respectively.

8 Conclusions

A new set of orbital elements for the numerical propagation of the perturbed two-body problem has been presented. The new scheme, called Dromo(P), can be seen as a generalization of the element method published by Peláez et al. in 2007 with an improved performance for the case when perturbations arise partially or totally from a potential. As such, the scheme inherits all the benefits of Peláez's method, among which it is notable that it can propagate different conics without resorting to Stumpff functions. Moreover, it is shown that the singularity that affects Peláez's method for the case of vanishing angular momentum is removed in the proposed method. Numerical tests with astrodynamics problems widely used in the literature, namely the propagation of elliptic orbits under J_2 perturbation applied alone and together with either lunar attraction or atmospheric drag, have been performed highlighting the excellent performance of the method. More specifically, when considering as a performance metric the achievable accuracy per number of function calls required and as a numerical integrator the explicit Runge–Kutta (4, 5) pair of Dormand and Prince known as DOPRI5, the proposed method behaves always better than Peláez's scheme, and the improvement in the performance increases as perturbations derived from a potential, the J_2 in our examples, have a stronger effect on the motion. In fact for the case of near circular motion perturbed by J_2 and either third body attraction or drag Dromo(P) not only ranks first among the compared methods but also transforms the growth of the position error over the independent variable from quadratic to linear. Similar conclusions are drawn also when the explicit Runge-Kutta code of order 8 based on the method of Dormand and Prince is employed [4].

An important role is played in our comparisons by the error accumulated in the physical time, which can become dominant over the error affecting the generalized orbital elements. We have shown that if the physical time is propagated with a much higher accuracy than is achievable by adopting a time transformation of Sundman type, Dromo(P) further gains in performance with respect to Dromo and the other formulations even when forces arising from a potential exert a moderate influence on the motion. For this reason the development of a time-element for Dromo(P) is currently under investigation and will be presented in a forthcoming paper.

Acknowledgments The study has been supported by the research project "Dynamic Simulation of Complex Space Systems" supported by the Dirección General de Investigación of the (former) Spanish Ministry of Innovation and Science through contract AYA2010-18796.

9 Appendix I

9.1 Matrices $Q_{\mathcal{RI}}$ and Q_0

We write below the expressions of the elements of the matrix $Q_{\mathcal{RI}}$:

$$Q_{\mathcal{RI}}(1,1) = \frac{R_X}{r},$$
$$Q_{\mathcal{RI}}(2,1) = \frac{R_Y}{r},$$
$$Q_{\mathcal{RI}}(3,1) = \frac{R_Z}{r},$$
$$Q_{\mathcal{RI}}(1,2) = \frac{H_Y R_Z - H_Z R_Y}{hr},$$

[4] This is the numerical integrator DOP853 which is described in Section II.5 of Hairer et al. (2009).

$$
\begin{aligned}
Q_{\mathcal{RI}}(2,2) &= \frac{H_Z R_X - H_X R_Z}{hr},\\
Q_{\mathcal{RI}}(3,2) &= \frac{H_X R_Y - H_Y R_X}{hr},\\
Q_{\mathcal{RI}}(1,3) &= \frac{H_X}{h},\\
Q_{\mathcal{RI}}(2,3) &= \frac{H_Y}{h},\\
Q_{\mathcal{RI}}(3,3) &= \frac{H_Z}{h}.
\end{aligned}
$$

We write below the expressions of the elements of the matrix Q_0:

$$
\begin{aligned}
Q_0(1,1) &= \frac{R_X}{r}\cos\triangle\phi - \left(\frac{H_Y R_Z - H_Z R_Y}{hr}\right)\sin\triangle\phi,\\
Q_0(2,1) &= \frac{R_Y}{r}\cos\triangle\phi - \left(\frac{H_Z R_X - H_X R_Z}{hr}\right)\sin\triangle\phi,\\
Q_0(3,1) &= \frac{R_Z}{r}\cos\triangle\phi - \left(\frac{H_X R_Y - H_Y R_X}{hr}\right)\sin\triangle\phi,\\
Q_0(1,2) &= \frac{R_X}{r}\sin\triangle\phi + \left(\frac{H_Y R_Z - H_Z R_Y}{hr}\right)\cos\triangle\phi,\\
Q_0(2,2) &= \frac{R_Y}{r}\sin\triangle\phi + \left(\frac{H_Z R_X - H_X R_Z}{hr}\right)\cos\triangle\phi,\\
Q_0(3,2) &= \frac{R_Z}{r}\sin\triangle\phi + \left(\frac{H_X R_Y - H_Y R_X}{hr}\right)\cos\triangle\phi,\\
Q_0(1,3) &= \frac{H_X}{h},\\
Q_0(2,3) &= \frac{H_Y}{h},\\
Q_0(3,3) &= \frac{H_Z}{h}.
\end{aligned}
$$

9.2 Expressions of ζ_4, ζ_5 and ζ_6 when $\zeta_7 = 0$

In the case that $\zeta_7 = 0$ Eqs. (55)–(57) become singular and we can use instead:

$$\zeta_4 = \frac{Q_0(1,3)}{2\zeta_6}, \tag{69}$$

$$\zeta_5 = \frac{Q_0(2,3)}{2\zeta_6}, \tag{70}$$

$$\zeta_6 = \pm\sqrt{\frac{Q_0(3,3)+1}{2}}.$$

If additionally $\zeta_6 = 0$ Eqs. (69) and (70) are singular and we can use instead:

$$\zeta_4 = \pm\sqrt{\frac{1 - Q_0(2,2)}{2}}, \qquad \zeta_5 = \frac{Q_0(1,2)}{2\zeta_4}.$$

Finally, if also $\zeta_4 = 0$, then we have $\zeta_5 = \pm 1$.

References

Arakida, H., Fukushima, T.: Long-term integration error of Kustaanheimo-Stiefel regularized orbital motion. Astron. J. **120**(6), 3333–3339 (2000)

Arakida, H., Fukushima, T.: Long-term integration error of Kustaanheimo-Stiefel regularized orbital motion. II. Method of variation of parameters. Astron. J. **121**(3), 1764–1767 (2001)

Battin, R.H.: An Introduction to the Mathematics and Methods of Astrodynamics. AIAA Education Series, AIAA, Reston, VA (1999)

Bombardelli, C., Baù, G., Peláez, J.: Asymptotic solution for the two-body problem with constant tangential thrust acceleration. Celest. Mech. Dyn. Astron **110**(3), 239–256 (2011)

Bond, V.R.: The uniform, regular differential equations of the KS transformed perturbed two-body problem. Celest Mech **10**(3), 303–318 (1974)

Bond, V.R.: Error propagation in the numerical solutions of the differential equations of orbital mechanics. Celest. Mech. **27**, 65–77 (1982)

Bond, V.R., Allman, M.C.: Modern Astrodynamics: Fundamentals and Perturbation Methods. Princeton University Press, Princeton (1996)

Burdet, C.A.: Regularization of the two body problem. Zeitschrift für angewandte Mathematik und Physik **18**(3), 434–438 (1967)

Burdet, C.A.: Theory of Kepler motion: the general perturbed two body problem. Zeitschrift für angewandte Mathematik und Physik **19**(2), 345–368 (1968)

Burdet, C.A.: Le mouvement Keplerien et les oscillateurs harmoniques. Journal für die reine und angewandte Mathematik **238**, 71–84 (1969)

Chelnokov, Y.N.: Application of quaternions in the theory of orbital motion of a satellite. I. Cosmic Res **30**(6), 612–621 (1993)

Deprit, A.: Ideal elements for perturbed Keplerian motions. J. Res. Natl. Bur Standards **79B**(1–2), 1–15 (1975)

Deprit, A., Elipe, A., Ferrer, S.: Linearization: Laplace vs. Stiefel. Celest. Mech. Dyn. Astron. **58**(2), 151–201 (1994)

Ferrándiz, J.M.: A general canonical transformation increasing the number of variables with application in the two-body problem. Celest. Mech. **41**(1–4), 343–357. (1987/1988)

Fukushima, T.: New two-body regularization. Astron. J. **133**(1), 1–10 (2007a)

Fukushima, T.: Numerical comparison of two-body regularizations. Astron. J. **133**(6), 2815–2824 (2007b)

Hairer, E., Nørsett, S.P., Wanner, G.: Solving Ordinary Differential Equations I: Nonstiff Problems, vol. 1. Springer, Berlin (2009)

Hansen, P.A.: Auseinandersetzung einer Zweckmässigen Methode zur Berechnung der absoluten Störungen der Kleinen Planeten. Abh der Math-Phys Cl der Kon Sachs Ges der Wissensch **5**, 41–218 (1857)

Kustaanheimo, P., Stiefel, E.L.: Perturbation theory of Kepler motion based on spinor regularization. Journal für die reine und angewandte Mathematik **218**, 204–219 (1965)

Levi-Civita, T.: Questioni di meccanica classica e relativista. Zanichelli, Bologna (1924)

Peláez, J., Hedo, J.M., de Andrés, P.R.: A special perturbation method in orbital dynamics. In: Proceedings of the AAS/AIAA Space Flight Mechanics Meeting held January 23–27, 2005, Copper Mountain, Colorado, American Astronautical Society, Univelt, Inc., San Diego, CA, pp 1061–1078 (2005)

Peláez, J., Hedo, J.M., de Andrés, P.R.: A special perturbation method in orbital dynamics. Celest. Mech. Dyn. Astron. **97**(2), 131–150 (2007)

Sharaf, M.A., Awad, M.E., Najmuldeen, S.A.A.: Motion of artificial satellites in the set of Eulerian redundant parameters (III). Earth Moon Planets **56**(2), 141–164 (1992)

Sperling, H.: Computation of Keplerian Conic sections. Am. Rocket Soc. J. **31**(5), 660–661 (1961)

Stiefel, E.L., Scheifele, G.: Linear and Regular Celestial Mechanics. Springer, New York (1971)

Stiefel, E., Rössler, M., Waldvogel, J., Burdet, C.A.: Methods of Regularization for Computing Orbits in Celestial Mechanics. Technical report, NASA CR-769, Washington, DC (1967)

Sundman, K.F.: Recherches sur le problème des trois corps. Acta Societatis Scientiarum Fennicae **34**(6), 1–43 (1907)

Sundman, K.F.: Mémoire sur le problème des trois corps. Acta Mathematica **36**(1), 105–179 (1912)

Szebehely, V.: Regularization in celestial mechanics. In: Oden J (ed) Computational Mechanics, Lecture Notes in Mathematics, vol 461, Springer, Berlin, pp 257–263, http://dx.doi.org/10.1007/BFb0074156 (1975)

Szebehely, V., Bond, V.: Transformations of the perturbed two-body problem to unperturbed harmonic oscillators. Celest. Mech. **30**, 59–69 (1983)

Vallado, D.A.: Fundamentals of Astrodynamics and Applications, 2nd edn. Kluwer Academic Publishers, Dordrecht (2001)